

THEORETICAL CORRELATION OF THE GEOMETRY AND  
MAGNETIC HYPERFINE SPLITTINGS OF THE METHYL RADICAL

Thesis by  
Robert Frank

In partial fulfillment of the requirements for  
the degree of  
Master of Science

California Institute of Technology  
Pasadena, California

1970

(Submitted August 20, 1969)

To My Parents

#### ACKNOWLEDGEMENTS

I wish to thank Dr. William A. Goddard, III, for his warm encouragement and enthusiastic counsel.

Many of the calculations described herein depended on computer programs written by Dr. Goddard, Dr. Russell Pitzer, Dr. William Palke, Steven Guberman, and David Huestis.

The typing was kindly and patiently undertaken by Marian Henneman.

## ABSTRACT

Spin densities at carbon and hydrogen are calculated at several out of plane angles of the methyl radical. Comparison with temperature dependent ESR studies indicate that the GF method describes the variation adequately while Hartree-Fock, Unrestricted Hartree-Fock, and Valence-Bond treatments do not.

The near planarity of the methyl radical is well documented, both experimentally<sup>1,2,3</sup> and theoretically.<sup>4,5,6</sup> Electron spin resonance studies of the hyperfine splittings of  $\cdot\text{CH}_3$  and its isotopic analogues,<sup>3</sup> and the temperature dependence of these splittings,<sup>7</sup> have characterized the changes in spin density at the nuclei that accompany symmetric out-of-plane bending of the radical. It is found that, as the reduced mass increases, the  $\text{C}^{13}$  splitting decreases, indicating that the spin density at the carbon atom is enhanced by greater vibrational frequencies. The opposite effect is observed on the magnitude of the spin densities at the hydrogen isotopes. Milligan and Jacox<sup>2</sup> have suggested that a "negative anharmonic" term in the potential may be important for interpreting isotopic shifts in the infrared spectrum. Because this quartic correction has the same sign as the quadratic term in the potential, an essentially planar structure is required, and deviations from planarity increase with increasing vibrational frequency. Open-shell Hartree-Fock (HF),<sup>4,5</sup> Unrestricted Hartree-Fock (UHF),<sup>4</sup> and semi-empirical Valence Bond (VB)<sup>6</sup> calculations agree qualitatively with these results. Because the reported HF and UHF wave functions are expressed in terms of Gaussian functions, they cannot be expected to yield accurate spin densities.<sup>9</sup> Schrader's recent VB calculation<sup>8</sup> predicts values for the temperature coefficients of the hyperfine splitting,  $(d |a_{\text{H}}| / dT)$  and  $(d |a_{\text{D}}| / dT)$ , that are significantly smaller than the experimental values. Possibly, this is due to the negligible effect of the VB  $\pi$  orbital on the hydrogen spin densities, even for non-planar geometries. HF, UHF, PUHF, and GF calculations have been done, using a small basis set of Slater orbitals, in order to examine the reliability of these methods, to attempt to remove the discrepancy between experiment and theory, and to offer a rationale for why the planar geometry should be energetically most favorable.

It has been shown previously how to construct variationally optimized many-electron GF wave functions, that are eigenfunctions of  $S^2$  and satisfy Pauli's Principle.<sup>10</sup> These wave functions describe molecular dissociation properly,<sup>10a</sup> predict the stability of anions with a loosely bound outer electron,<sup>10b</sup> and yield interpretable values for spin densities.<sup>10c</sup> Such favorable qualities suggest that useful correlations between the hyperfine splitting constants and structure may be realized using the GF method. This approach overemphasizes the splitting between orbitals with the same spatial quantum numbers, however.<sup>11</sup> This results because only one form of spin coupling is considered (out of 42 for a nine electron doublet), and that type effectively introduces triplet character into the inner cores.<sup>11</sup> An unbiased coupling can be achieved variationally by using SOGI<sup>12</sup> wave functions. UHF wave functions are not eigenfunctions of  $S^2$ , but they are completely optimized within the framework of representing a wave function by a single determinant of spin-orbitals. When these are projected (after optimization) to yield PUHF<sup>13</sup> results, the spin densities are found to have very nearly the same magnitude as the experimental values. None of these methods permits the relaxation of spatial symmetry requirements on the molecular orbitals necessary to account for angular correlation.

Localized orbitals provide a basis for an intuitive description of the nature of the potential and the changes in hyperfine coupling with angle. The localization procedure employed here, adapted by Guberman and Goddard<sup>14</sup> from Edmiston and Reudenberg's<sup>15</sup> localization technique for HF orbitals, minimizes the interorbital electron repulsion energy by applying appropriate unitary transformations to the a set of orbitals and to the b set. Non-unitary transformations and other weighting functions besides  $(r_{ij})^{-1}$  would produce different localized orbitals.

### CALCULATIONS

Approximate solutions to the GF equations were obtained at five out-of-plane angles (see Figure 1.) using the experimental bond length of 1.079 Å.<sup>16</sup> The wave functions were sought in terms of a set of nine Slater orbitals, the minimum number required for significant splitting to occur. The GF orbitals were restricted to be basis functions of irreducible representations of the point group C<sub>3</sub>. In the a set there result 3 orbitals of A symmetry and a pair with E symmetry. The b set lacks the  $\pi$  orbital of A symmetry. Table 1. lists the coefficients and orbital energies of the GF orbitals at the various angles considered. The LGF coefficients are collected in Table 2.

### DISCUSSION

The sum of the orbital energies of the a set remains essentially constant at all angles considered, while the corresponding sum over the b set changes markedly, at very nearly the same rate as the total energy. Both 1A orbitals are stabilized slightly as the out-of-plane angle increases, but the E pairs are destabilized. The splitting between the orbital energies of the 2A pair increases monotonically with angle, the a orbital energy increasing, the b orbital energy decreasing very slowly (see Figure 2). As the  $\pi$  orbital gains s character, its orbital energy is lowered. The fraction of s character can be represented as  $f_s = 2 \tan^2(\rho \theta)$ <sup>18</sup> where  $\rho$  is approximately .66, which is remarkably close to Fessenden's calculation of the experimental orbital following parameter, 0.648.<sup>3</sup> Because the symmetry properties of the GF eigenfunctions obscure their bonding properties, the spatial character of the orbitals is discussed in connection with LGF orbitals below.

Various energy quantities as a function of angle are listed in Table 3. A least squares fit of the total energy as a function of angle required the inclusion of a quartic term of the same sign as the quadratic term in order to yield an acceptable value of chi-squared. (See Table 4 for the coefficients.) The GF force constant is  $0.564 \text{ mdyne}/\text{\AA}^\circ$  in contrast to the experimental value of  $0.177 \text{ mdyne}/\text{\AA}^\circ$ .<sup>4</sup> Although the potential function calculated by Nesbet's modified HF method<sup>17</sup> closely parallels the GF potential, the UHF potential is very flat with a relatively large quartic character. From Figure 3, it is apparent that the increase in nuclear repulsion energy with angle is much more rapid than the corresponding increase in the total energy. Only the exchange kinetic energy  $T_x$  and the sum of the b set orbital energies, of all the quantities listed in Table 3, closely mimic the behavior of the total energy. (See Figure 3.) The use of changes in  $T_x$ , the total kinetic energy minus the trace of the kinetic energy matrix (the classical kinetic energy), as a criterion for understanding stability has been substantiated for small systems by Wilson and Goddard<sup>19</sup> within the framework of the GI method. Its extension from the treatment of energy variation with bond length to the study of energy changes with dihedral angle has also been attempted, notably in successfully calculating the barrier to rotation in ethane and dimethylacetylene. In relation to these barriers, it is interesting to note that the energy required to distort the methyl radical about  $2^\circ$  in the vicinity of the CCH angle in ethane corresponds to about half the barrier height. This suggests that optimizing the geometry of eclipsed  $\text{C}_2\text{H}_6$  may be necessary for understanding the redistribution of energy with an SCF model on going from the staggered to the eclipsed conformations.<sup>20</sup>

The interaction of nuclear spins and electron spins determines the magnetic hyperfine splitting. For liquids the only contribution to the splitting is from the isotropic Fermi contact term, which is



directly proportional to the spin density at the interacting nucleus,

$$a_N = c_N Q(0)$$

$$Q(0) = \frac{1}{\langle s_z \rangle} \langle \Psi | \sum_{\kappa} \delta(\vec{r}_{\kappa} - \vec{r}_N) s_{\kappa z} | \Psi \rangle$$

$Q(0)$  is the spin density at the nucleus N and  $a_N$  is the isotropic hyperfine splitting constant. See the Appendix for an explanation of the other parameters and the expression for  $Q(0)$ . Table 5 lists the values of  $Q(0)$  at several out-of-plane angles calculated with the GF, UHF, and PUHF approaches. In all cases the spin density at carbon is positive and increases with angle, while the spin density at hydrogen is negative and becomes less so with angle, in agreement with experiment.<sup>22</sup> Only the PUHF spin densities are comparable with experiment, however, the UHF values being three times too large and the GF values being four to five times too large. (Table 6 contains several experimental results.) The UHF and PUHF spin density variation with angle is much larger than the GF angle dependence.

Assuming a Boltzmann distribution of vibrational states, the applicability of the Born-Oppenheimer approximation, neglecting vibrational modes other than  $A_2''$ , neglecting vibrational states with more than two quanta of excitation, and using a force constant of .16 mdynes/Å,  $\langle a_H \rangle$  and  $\langle a_D \rangle$  and their temperature coefficients were calculated. At 0° K, the GF value of  $\langle a_H \rangle$  is 96.3 Gauss and of  $\langle a_D \rangle' = (g_H/g_D) \langle a_D \rangle$ , 97.1 Gauss. Although these values are much larger than the experimental values<sup>3</sup> of 23.038 and 23.295 (at 97° K), the theoretical ratio  $\langle a_H \rangle / \langle a_D \rangle'$  of .992 is only slightly larger than the experimental ratio of .9890±.0013. For CH<sub>3</sub> the calculated temperature coefficient at 273° K is +4.1 mGauss/°K (experimental<sup>7</sup>, 2.1±.2); for CD<sub>3</sub>, the calculated temperature coefficient of  $\langle a_D \rangle'$  is +5.5 mGauss/°K (experimental<sup>7</sup>, 2.3 mGauss/°K).

The theoretical ratio of 1.34 is considerably larger than the experimental value of 1.09. The UHF and PUHF methods cannot yield as good results for the ratios since the spin density variation with angle is so very much larger than what the GF method predicts.

Although it has been pointed out that GF spin densities are very sensitive to the choice of basis set,<sup>11</sup> whether the rate of change of spin density with bond angle is basis set dependent has not yet been determined. Nonetheless, an examination of the contribution to the spin density from each orbital pair will be undertaken to isolate the changes in spin density that occur with out-of-plane vibrations. The spin density can be written (see Appendix)

$$Q(0) = \frac{1}{q} \sum_{i=1}^5 q'_i = \sum_{i=1}^5 q_i$$

The  $q_i$  are collected in Table 7 for the angles considered. The contribution to  $Q(0)$  at C from the (a2A,b2A) core polarization predominates at all angles though its value decreases only moderately with angle. It is the increasing S character of the orbital with angle that leads to increased spin density at carbon. The correct interplay between these two contributions is demonstrated by the value of  $\rho$  stated above and the calculated value of the quadratic coefficient in the angular dependence of the carbon hyperfine coupling; the two experimental values<sup>3</sup> of 997 and 1265 bracket the GF value of 1100. For the planar radical, the valence (aE<sub>y</sub>,bE<sub>y</sub>) pair is largely responsible for the splitting at H<sub>1</sub>. Since the a orbital is centered primarily on carbon, while the b orbital is on the hydrogen, the spin density is negative. Because the contribution of this pair is insensitive to angle, as the out-of-plane angle increases, only two factors determine the decrease in the magnitude of  $Q(0)$  at the hydrogens: (1) the positive spin density of the  $\pi$  orbital becomes larger at the hydrogens as they move out of plane, and (2) the splitting of the valence pair (a2A,b2A) decreases with angle with a subsequent decrease in their amplitude difference at the hydrogens.

The (a<sub>1</sub>A, b<sub>1</sub>A) pair of LGF core orbitals are centered primarily on the carbon atom and retain more than 90% 1s character for all the angles considered. The remaining A orbitals are directed towards the vertices of a pyramidal structure with the  $\pi$  orbital along the C<sub>3</sub>-axis of  $\cdot\text{CH}_3$  and the projection of the remaining a  $\sigma$  orbitals along the carbon-hydrogen lines. For the planar geometry the  $\sigma$ - $\pi$  angle calculated at the carbon atom is 110.2°. This angle increases roughly like the square root of the angular deviation from planarity to 112.4° when  $\Theta=6^\circ$ . These deviations thus force the bonding a orbitals into a more closed arrangement.

In contrast, the three b orbitals are directed towards the vertices of an equilateral triangle and are centered mainly on the hydrogens. Instead of being directed more out of plane than the C-H lines, they lag behind the hydrogens by slightly more than half of  $\Theta$ . (This observation is of questionable value since these bent  $\sigma$ -bonds have relatively small amplitudes on the carbon, where the angle is calculated.)

Using localized HF orbitals, Kaldor<sup>21</sup> has shown that the  $\sigma$ - $\pi$  interactions of ammonia are affected most strongly and favorably on going from the planar to the pyramidal configuration. In addition, the bending of the bonds is far less for the pyramidal than for the planar structure. For the CH<sub>3</sub> LGF orbitals, it is found that the two electron repulsion matrix over the b orbitals is almost invariant to angle changes. Most of the changes occur in the corresponding matrix over the a orbitals (see Table 3.).

## CONCLUSIONS

None of the SCF methods considered yields accurate potential functions for the out-of-plane vibrational mode. Despite its over-emphasis of core polarization, the GF method predicts the angle dependence of the spin densities quite accurately. HF, UHF, PUHF, and VB methods do not. Further GF calculations with larger basis sets should be carried out in order to investigate the possibility that the above results are basis set dependent.

Contrary to Schrader's conclusion, which has been used to interpret the experimental results of Garbutt et al., the GF method predicts that the  $\pi$  electron does contribute greatly to the angle dependence of the proton hyperfine splitting.

Using different orbitals for different spins results in two sets of localized orbitals. One set of valence orbitals located mainly on carbon describes a pyramid; the other set, centered on the hydrogens, describes a triangle. Deviations from planarity increase the exchange kinetic energy and the sum of the b set orbital energies at approximately the same rate as the total energy.

APPENDIX

In the strong field limit the Fermi contact Hamiltonian is,

$$H_c = g_e \mu_B g_N \mu_N \frac{8\pi}{3} \sum_k \delta(\vec{r}_k - \vec{r}_N) s_{kz} I_{Nz}$$

where  $\mu_B$  and  $\mu_N$  are the Bohr and nuclear magnetons,  $g_e$  and  $g_N$  are the electron and nuclear g factors,  $\delta$  is the Dirac delta function, and  $s_{kz}$  and  $I_{Nz}$  are the z components of spin of electron k and nucleus N. Averaging over the approximate wave function  $\Psi$ , the first order perturbation correction to the energy is

$$\langle \Psi | H_c | \Psi \rangle = a_N g_e \mu_B \langle S_z \rangle \langle I_{Nz} \rangle$$

where the hyperfine coupling constant  $a_N$  (in Gauss) is directly proportional to the spin density,  $Q(0)$ ,

$$a_N = \frac{8\pi}{3} g_N \mu_N Q(0) = C_N Q(0)$$

$$Q(0) = \frac{1}{\langle S_z \rangle} \langle \Psi | \sum_k \delta(\vec{r}_k - \vec{r}_N) s_{kz} | \Psi \rangle$$

In order that  $Q(0)$  be in atomic units, the factor  $(a_0)^{-3}$  is absorbed into  $C_N$ . ( $a_0$  is the Bohr radius.)

The  $\cdot\text{CH}_3$  spin density calculated with a GF wave function can be expressed in the following form<sup>11</sup>:

$$\begin{aligned} Q(0) &= \frac{1}{9} \sum_{i=1}^4 \{ 4 \phi_{ia}^2(0) - 2 \phi_{ia}(0) \phi_{ib}(0) + 2 \phi_{ib}^2(0) \} \\ &\quad + \frac{1}{9} \phi_{5a}^2(0) \\ &= \frac{1}{9} \sum_{i=1}^5 q_i' = \sum_{i=1}^5 p_i \end{aligned}$$

TABLE 1.  $\cdot\text{CH}_3$  GF ORBITALS

PLANAR CONFIGURATION							
	EXPONENTS	1A1	2A1	3A1( $\pi$ )	$E_x$	$E_y$	
<u>a orbitals</u>							
H <sub>1</sub>	1s	1.206	-0.00153	-0.12184	0.0	0.0	0.33775
H <sub>2</sub>	1s	1.206	-0.00153	-0.12184	0.0	0.29250	-0.16888
H <sub>3</sub>	1s	1.206	-0.00153	-0.12184	0.0	-0.29250	-0.16888
C	1s	5.33	0.89684	0.28833	0.0	0.0	0.0
	1s'	8.66	0.10891	-0.02463	0.0	0.0	0.0
	2s	1.78	0.00989	-0.84750	0.0	0.0	0.0
	2 <sub>p<sub>z</sub></sub>	1.67	0.0	0.0	1.0	0.0	0.0
	2 <sub>p<sub>x</sub></sub>		0.0	0.0	0.0	0.71306	0.0
	2 <sub>p<sub>y</sub></sub>		0.0	0.0	0.0	0.0	0.71306
	Orbital energy		-11.2575	-1.0169	-0.3954	-0.58224	-0.58224
<u>b orbitals</u>							
H <sub>1</sub>	1s		0.00145	-0.34429		0.0	0.62027
H <sub>2</sub>	1s		0.00145	-0.34429		0.53717	-0.31013
H <sub>3</sub>	1s		0.00145	-0.34429		-0.53717	-0.31013
C	1s		0.89885	0.19981		0.0	0.0
	1s'		0.10921	-0.01447		0.0	0.0
	2s		-0.00067	-0.40350		0.0	0.0
	2 <sub>p<sub>z</sub></sub>		0.0	0.0		0.0	0.0
	2 <sub>p<sub>x</sub></sub>		0.0	0.0		0.39814	0.0
	2 <sub>p<sub>y</sub></sub>		0.0	0.0		0.0	0.39814
	Orbital energy		-11.1900	-0.8227		-0.5627	-0.5627

TABLE 1. (CONTINUED)

DEVIATION FROM PLANARITY = 2°						
		1A1	2A1	3A1( $\pi$ )	E <sub>x</sub>	E <sub>y</sub>
<u>a</u> orbitals						
H <sub>1</sub>	1s	-0.00153	-0.12183	0.01262	0.0	0.33780
H <sub>2</sub>	1s	-0.00153	-0.12183	0.01262	0.29254	-0.16890
H <sub>3</sub>	1s	-0.00153	-0.12183	0.01262	-0.29254	-0.16890
C	1s	0.89684	0.28833	0.00318	0.0	0.0
	1s'	0.10892	-0.02463	-0.00039	0.0	0.0
	2s	0.00989	-0.84753	-0.02005	0.0	0.0
	2 <sub>p<sub>z</sub></sub>	0.00011	0.00824	0.99922	0.0	0.0
	2 <sub>p<sub>x</sub></sub>	0.0	0.0	0.0	0.71314	0.0
	2 <sub>p<sub>y</sub></sub>	0.0	0.0	0.0	0.0	0.71314
	Orbital energy	-11.2576	-1.01657	-0.39575	-0.58214	-0.58214
<u>b</u> orbitals						
H <sub>1</sub>	1s	0.00145	-0.34394		0.0	0.62041
H <sub>2</sub>	1s	0.00145	-0.34394		0.53729	-0.31020
H <sub>3</sub>	1s	0.00145	-0.34394		-0.53729	-0.31020
C	1s	0.89886	0.19986		0.0	0.0
	1s'	0.10921	-0.01448		0.0	0.0
	2s	-0.00067	-0.40392		0.0	0.0
	2 <sub>p<sub>z</sub></sub>	0.00000	-0.00965		0.0	0.0
	2 <sub>p<sub>x</sub></sub>	0.0	0.0		0.39818	0.0
	2 <sub>p<sub>y</sub></sub>	0.0	0.0		0.0	0.39818
	Orbital energy	-11.1901	-0.8229		-0.5625	-0.5625

TABLE 1. (CONTINUED)

		DEVIATION FROM PLANARITY = $4^\circ$				
		1A	2A	3A( $\pi$ )	$E_x$	$E_y$
<u>a</u> orbitals						
H <sub>1</sub>	1s	-0.00152	-0.12181	0.02512	0.29269	0.33797
H <sub>2</sub>	1s	-0.00152	-0.12181	0.02512	-0.29269	-0.16899
H <sub>3</sub>	1s	-0.00152	-0.12181	0.02512	0.0	-0.16899
C	1s	0.89683	0.28832	0.00632	0.0	0.0
	1s'	0.10893	-0.02463	-0.00077	0.0	0.0
	2s	0.00984	-0.84757	-0.03991	0.0	0.0
	2 <sub>p<sub>z</sub></sub>	0.00022	0.01645	0.99692	0.0	0.0
	2 <sub>p<sub>x</sub></sub>	0.0	0.0	0.0	0.71338	0.0
	2 <sub>p<sub>y</sub></sub>	0.0	0.0	0.0	0.0	0.71338
	Orbital energy	-11.2580	-1.0156	-0.3969	-0.5818	-0.5818
<u>b</u> orbitals						
H <sub>1</sub>	1s	0.00143	-0.34290		0.0	0.62082
H <sub>2</sub>	1s	0.00143	-0.34290		0.53764	-0.31041
H <sub>3</sub>	1s	0.00143	-0.34290		-0.53764	-0.31041
C	1s	0.89886	0.20003		0.0	0.0
	1s'	0.10919	-0.01452		0.0	0.0
	2s	-0.00064	-0.40523		0.0	0.0
	2 <sub>p<sub>z</sub></sub>	-0.00001	-0.01817		0.0	0.0
	2 <sub>p<sub>x</sub></sub>	0.0	0.0		0.39833	0.0
	2 <sub>p<sub>y</sub></sub>	0.0	0.0		0.0	0.3933
	Orbital energy	-11.1905	-0.8236		-0.5618	-0.5618



TABLE 1. (CONTINUED)

DEVIATION FROM PLANARITY = 6°						
		1A	2A	3A( $\pi$ )	$E_x$	$E_y$
<u>a orbitals</u>						
H <sub>1</sub>	1s	-0.00151	-0.12176	0.03737	0.0	0.33825
H <sub>2</sub>	1s	-0.00151	-0.12176	0.03737	0.29294	-0.16913
H <sub>3</sub>	1s	-0.00151	-0.12176	0.03737	-0.29294	-0.16913
C	1s	0.89682	0.28828	0.00941	0.0	0.0
	1s'	0.10896	-0.02460	-0.00115	0.0	0.0
	2s	0.00980	-0.84768	-0.05936	0.0	0.0
	2 <sub>p<sub>z</sub></sub>	0.00033	0.02459	0.99314	0.0	0.0
	2 <sub>p<sub>x</sub></sub>	0.0	0.0	0.0	0.71378	0.0
	2 <sub>p<sub>y</sub></sub>	0.0	0.0	0.0	0.0	0.71378
	Orbital energy	-11.2587	-1.0141	-0.39874	-0.58132	-0.58132
<u>b orbitals</u>						
H <sub>1</sub>	1s	0.00141	-0.34120		0.0	0.62149
H <sub>2</sub>	1s	0.00141	-0.34120		0.53823	-0.31075
H <sub>3</sub>	1s	0.00141	-0.34120		-0.53823	-0.31075
C	1s	0.89888	0.20031		0.0	0.0
	1s'	0.10917	-0.01460		0.0	0.0
	2s	-0.00059	-0.40730		0.0	0.0
	2 <sub>p<sub>z</sub></sub>	-0.00000	-0.02742		0.0	0.0
	2 <sub>p<sub>x</sub></sub>	0.0	0.0		0.39859	0.0
	2 <sub>p<sub>y</sub></sub>	0.0	0.0		0.0	0.39859
	Orbital energy	-11.1911	-0.8247		-0.5607	-0.5607

TABLE 1. (CONTINUED)

DEVIATION FROM PLANARITY = 12°						
		1A	2A	3A( $\pi$ )	$E_x$	$E_y$
<u>a</u> orbitals						
H <sub>1</sub>	1s	-0.00014	0.12146	0.07163	0.0	0.33941
H <sub>2</sub>	1s	-0.00014	0.12146	0.07163	0.29394	-0.16970
H <sub>3</sub>	1s	-0.00014	0.12146	0.07163	-0.29394	-0.16970
C	1s	0.89674	-0.28817	0.01808	0.0	0.0
	1s'	0.10910	0.02451	-0.00222	0.0	0.0
	2s	0.00955	0.84831	-0.11388	0.0	0.0
	2p <sub>z</sub>	0.00061	-0.04808	0.97406	0.0	0.0
	2p <sub>x</sub>	0.0	0.0	0.0	0.71634	0.0
	2p <sub>y</sub>	0.0	0.0	0.0	0.0	+0.71634
	Orbital energy	-11.2620	-1.0065	-0.40847	-0.57836	-0.57836
<u>b</u> orbitals						
H <sub>1</sub>	1s	0.00128	0.33259		0.0	0.62542
H <sub>2</sub>	1s	0.00128	0.33259		0.54163	-0.31271
H <sub>3</sub>	1s	0.00128	0.33259		-0.54163	-0.31271
C	1s	0.89894	-0.20151		0.0	0.0
	1s'	0.10907	0.01496		0.0	0.0
	2s	-0.00036	0.41725		0.0	0.0
	2p <sub>z</sub>	0.00002	0.05632		0.0	0.0
	2p <sub>x</sub>	0.0	0.0		0.39975	0.0
	2p <sub>y</sub>	0.0	0.0		0.0	0.39975
	Orbital energy	-11.1940	-0.8308		-0.5547	-0.5547

TABLE 2.  $\cdot\text{CH}_3$  IGF ORBITALS

		DEVIATION FROM PLANARITY = $0^\circ$				
		CORE A	A $\sigma_1$	A $\pi$	CORE B	B $\sigma_1$
H <sub>1</sub>	1s	-0.01791	0.34037	0.04479	-0.02697	0.70462
H <sub>2</sub>	1s	-0.01791	-0.07328	0.04479	-0.02697	-0.05506
H <sub>3</sub>	1s	-0.01791	-0.07328	0.04479	-0.02697	-0.05506
C	1s	0.92748	-0.08910	-0.05860	0.91228	-0.07214
	1s'	0.10461	0.02086	0.01485	0.10764	0.01353
	2s	-0.10422	0.45083	0.31265	-0.03397	0.23212
	2 <sub>p<sub>z</sub></sub>	-0.00327	-0.21482	0.92820	0.0	0.0
	2 <sub>p<sub>x</sub></sub>	0.0	0.0	0.0	0.0	0.0
	2 <sub>p<sub>y</sub></sub>	0.0	0.58222	0.0	0.0	0.32507

TABLE 2 . (CONTINUED)

DEVIATION FROM PLANARITY = 2°						
		CORE A	A $\sigma_i$	A $\pi$	CORE B	B $\sigma_i$
H <sub>1</sub>	1s	-0.01786	0.34251	-0.03654	-0.02695	0.70454
H <sub>2</sub>	1s	-0.01786	-0.07120	-0.03654	-0.02695	-0.05531
H <sub>3</sub>	1s	-0.01786	-0.07120	-0.03654	-0.02695	-0.05531
C	1s	0.92751	-0.08761	0.06448	0.91229	-0.07216
	1s'	0.10460	0.02046	-0.01648	0.10764	0.01354
	2s	-0.10450	0.44060	0.35429	-0.03400	0.23237
	2 <sub>p<sub>z</sub></sub>	0.00636	0.22641	0.91907	-0.00075	0.00521
	2 <sub>p<sub>x</sub></sub>	0.0	0.0	0.0	0.0	0.0
	2 <sub>p<sub>y</sub></sub>	0.0	0.58229	0.0	0.0	0.32511

TABLE 2. (CONTINUED)

DEVIATION FROM PLANARITY = $4^\circ$						
		CORE A	A $\sigma_r$	A $\pi$	CORE B	B $\sigma_r$
H <sub>1</sub>	1s	-0.01776	0.34516	-0.02795	-0.02690	0.70427
H <sub>2</sub>	1s	-0.01776	-0.06875	-0.02795	-0.02690	-0.05609
H <sub>3</sub>	1s	-0.01776	-0.06875	-0.02795	-0.02690	-0.05609
C	1s	0.92755	-0.08626	0.06940	0.91231	-0.07221
	1s'	0.10461	0.02010	-0.01786	0.10762	0.01358
	2s	-0.10483	0.43075	0.39042	-0.03412	0.23313
	2p <sub>z</sub>	0.00936	0.23432	0.91067	-0.00151	0.01045
	2p <sub>x</sub>	0.0	0.0	0.0	0.0	0.0
	2p <sub>y</sub>	0.0	0.58249	0.0	0.0	0.32522

TABLE 2. (CONTINUED)

		DEVIATION FROM PLANARITY = 6°				
		CORE A	A $\sigma$	A $\pi$	CORE B	B $\sigma$
H <sub>1</sub>	1s	-0.01761	0.34814	-0.01936	-0.02682	0.70385
H <sub>2</sub>	1s	-0.01761	-0.06612	-0.01936	-0.02682	-0.05734
H <sub>3</sub>	1s	-0.01761	-0.06612	-0.01936	-0.02682	-0.05734
C	1s	0.92757	-0.08496	0.07373	0.91236	-0.07232
	1s'	0.10463	0.01973	-0.01906	0.10759	0.01361
	2s	-0.10523	0.42118	0.42301	-0.03428	0.23431
	2 <sub>p<sub>z</sub></sub>	0.01224	0.23993	0.90226	-0.00227	0.01578
	2 <sub>p<sub>x</sub></sub>	0.0	0.0	0.0	0.0	0.0
	2 <sub>p<sub>y</sub></sub>	0.0	0.58281	0.0	0.0	0.32543

TABLE 3

	0°	2°	4°	6°	12°
Nuclear Repulsion Energy	9.67715	9.67767	9.67923	9.68183	9.69613
Kinetic Energy	39.63042	39.63069	39.63148	39.63284	39.64087
Electron- Nuclear Energy	-111.24434	-111.24495	-111.24678	-111.24998	-111.27011
Electron- Electron Repulsion	22.42060	22.42050	22.42028	22.42001	22.42110
Total Energy	-39.51617	-39.51608	-39.51580	-39.51530	-39.51202
Exchange Kinetic Energy	-0.09819	-0.09798	-0.09734	-0.09633	
Sum of Self- Repulsion Integrals					
<u>a</u> orbitals	6.35387	6.36365	6.37288	6.38139	
<u>b</u> orbitals	5.65287	5.65283	5.65273	5.65258	
Classical Kinetic Energy	39.72861	39.72866	39.72881	39.72916	
Virial Ratio	1.00145	1.00145	1.00146	1.00149	1.00163
Sum of <u>a</u> set Orbital Energies	-13.8343	-13.8342	-13.8341	-13.8342	-13.8337
Sum of <u>b</u> set Orbital Energies	-13.1381	-13.1380	-13.1377	-13.1372	-13.1342

TABLE 4. COEFFICIENTS IN  $E = c_0 + c_1 \theta^2 + c_2 \theta^4$

Method	$c_0$	$c_1$	$c_2$	Chi-Squared
GF	-39.51617587	0.07530892	0.44456232	$0.7 \times 10^{-12}$
UHF	-39.50125015	0.00564906	0.78962362	$0.2 \times 10^{-11}$
HF	-39.49471974	0.04905856	0.63049877	$1.0 \times 10^{-12}$



TABLE 5

SPIN DENSITY AT CARBON			
	GF	UHF	PUHF
0°	0.421965	.2568	.08943
2°	0.425321	.2607	.09764
4°	0.435071	.2721	.12176
6°	0.451804	.2907	.16039
12°	0.497578	.3816	.34144

SPIN DENSITY AT HYDROGEN			
	GF	UHF	PUHF
0°	-.062623	-.04923	-.01599
2°	-.062535	-.04896	-.01580
4°	-.062273	-.04817	-.01523
6°	-.061850	-.04692	-.01434
12°	-.059922	-.04158	-.01041

TABLE 6. EXPERIMENTAL RESULTS<sup>3\*</sup>

Radical	Spin Density at Proton	Spin Density at Carbon
$^{12}\text{CH}_3$	0.01444(23.038)	---
$^{13}\text{CH}_3$	0.01445(23.04)	0.0956(38.34)
$^{12}\text{CD}_3$	0.014605(3.576)	---
$^{13}\text{CD}_3$	0.014613(3.578)	0.0897(35.98)

\* Numbers in parentheses are hyperfine splitting constants in Gauss.

TABLE 7. CONTRIBUTION TO THE SPIN DENSITIES BY GF ORBITAL PAIRS

Angle	(a <sub>1A</sub> ,b <sub>1A</sub> )	(a <sub>2A</sub> ,b <sub>2A</sub> )	(aE <sub>x</sub> ,bE <sub>x</sub> )	(aE <sub>y</sub> ,bE <sub>y</sub> )	$\pi$
At H <sub>1</sub>					
0°	0.0	-0.018766	0.0	-0.043857	0.0
2°	0.0	-0.018711	0.0	-0.043878	0.000053
4°	0.0	-0.018544	0.0	-0.043939	0.000210
6°	0.0	-0.018274	0.0	-0.044040	0.000403
At C					
0°	-0.022520	0.444484	0.0	0.0	0.0
2°	-0.022117	0.442282	0.0	0.0	0.005156
4°	-0.020903	0.435601	0.0	0.0	0.020433
6°	-0.018820	0.425342	0.0	0.0	0.045282

FIGURE 1: THE COORDINATE SYSTEM USED

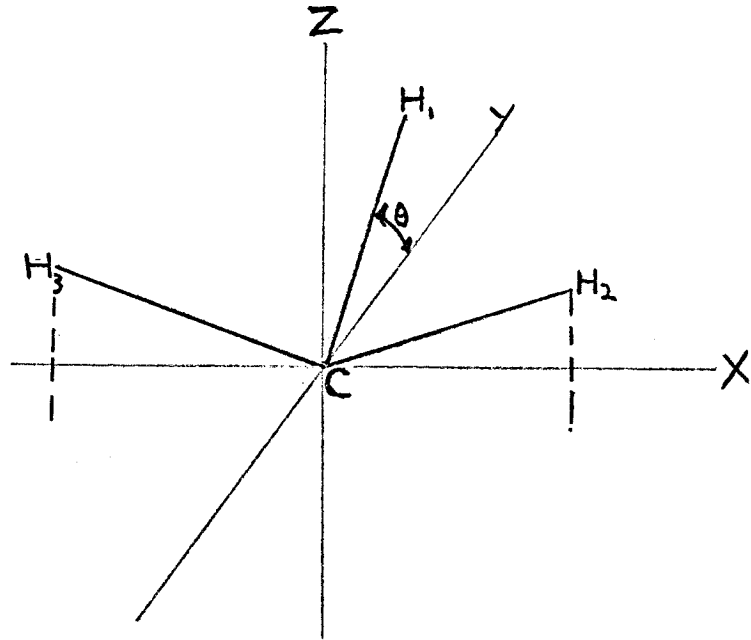


FIGURE 2: 2A ORBITAL ENERGIES (HARTREES) VERSUS ANGLE

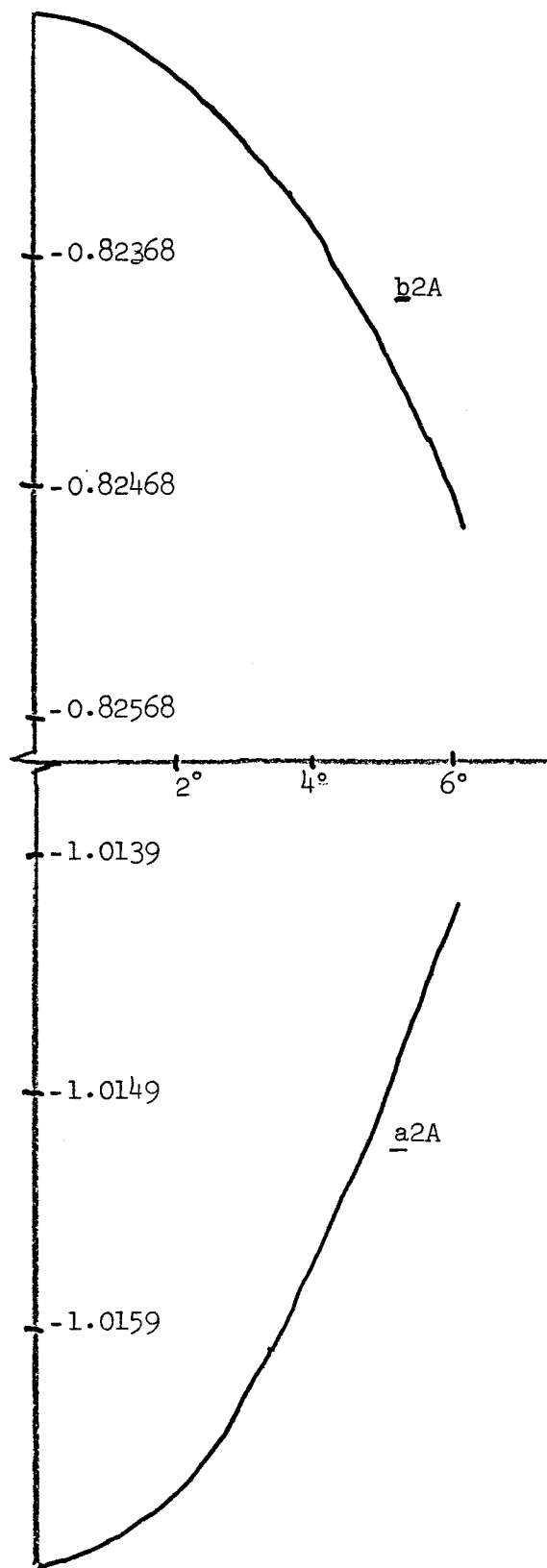
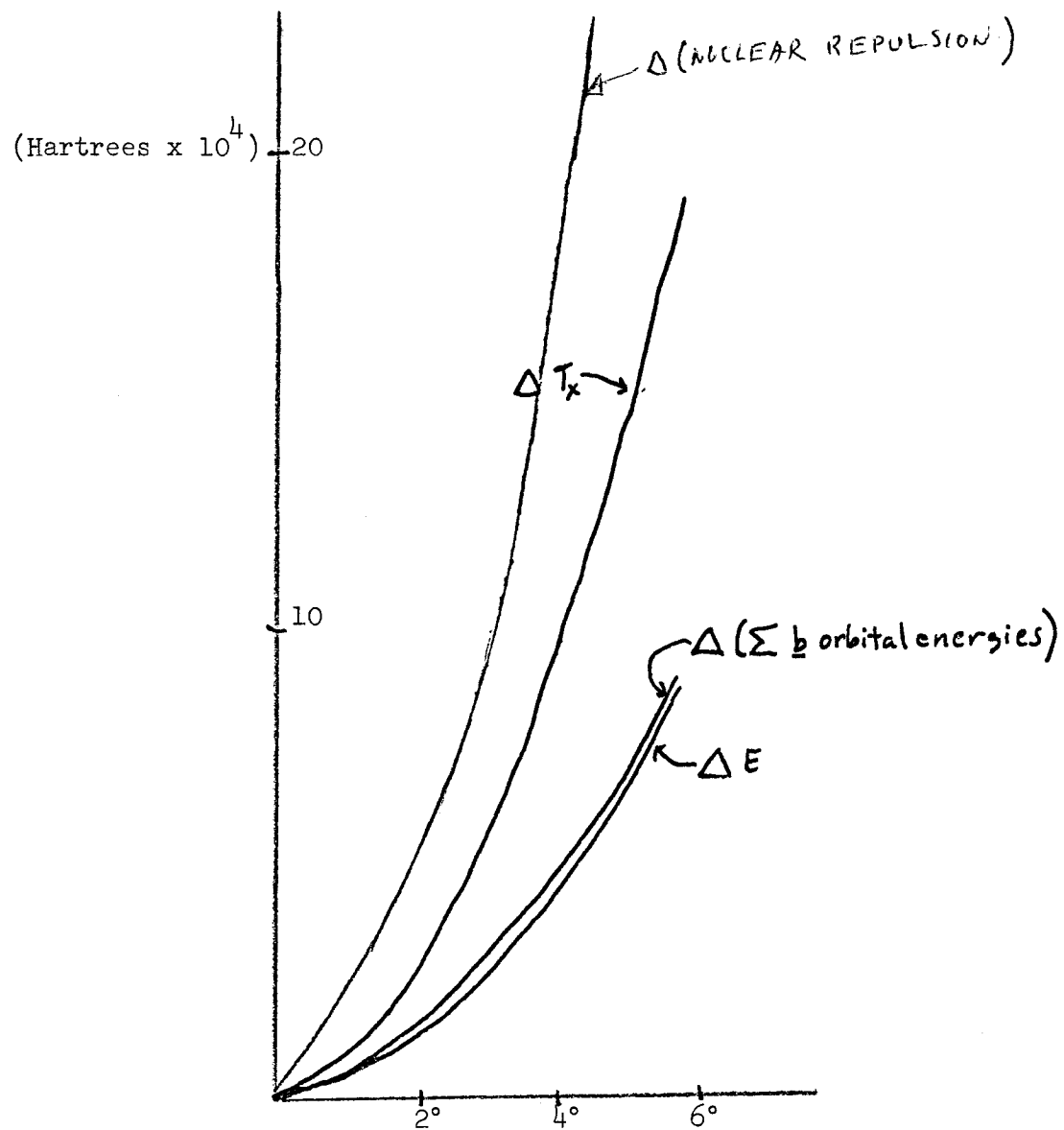


FIGURE 3: VARIATION OF CHANGES IN EXCHANGE KINETIC ENERGY, TOTAL ENERGY, AND SUM OF  $\underline{b}$  ORBITAL ENERGIES WITH ANGLE.



## REFERENCES

1. G. Herzberg, Proc. Roy. Soc. (London), A262, 291 (1961)
2. D. E. Milligan, M. E. Jacox, J. C. P., 47, 5146 (1967)
3. R. W. Fessenden, J. Phys. Chem., 71, 74 (1967)
4. K. Morokuma, L. Pederson, M. Karplus, J. C. P., 48, 4801 (1968)
5. P. Millie, G. Berthier, Int. J. Quant. Chem., IIs, 67 (1968)
6. M. Karplus, J. C. P., 30, 15 (1959)
7. G. B. Garbutt, H. D. Gesser, M. Fujimoto, Ibid., 48, 4605 (1968)
8. D. M. Schrader, Ibid., 46, 3895 (1967)
9. S. Huzinaga, Ibid., 42, 1293 (1965) and reference 11.
10. W. A. Goddard III, Phys. Rev., 157, 73, 81, 93, (1967);
  - 10a. J. C. P., 48, 5337;
  - 10b. Phys. Rev. 172, 7 (1968);
  - 10c. Ibid., 176, 106 (1968)
  - 10d. J. C. P., 48, 1008 (1968)
11. W. A. Goddard III, "Core Polarization and Hyperfine Structure of the B, C, N, O, and F Atoms" (to be published)
12. R. Ladner, W. A. Goddard III, "...The Spin-Coupling Optimized GI Method" (to be published)
13. See, for example, L. M. Sachs, Phys. Rev., 117, 1504 (1960)
14. S. L. Guberman, W. A. Goddard III, to be published
15. C. Edmiston, K. Reudenberg, Rev. Mod. Phys., 35, 457 (1963);  
J. C. P., S97 (1965)
16. Actually used 2.039 Rohr.
17. See, for example, R. K. Nesbet, J. C. P., 43, 4403 (1965)
18. D. M. Schrader, M. Karplus, J. C. P., 40, 1593 (1964)
19. C. W. Wilson, W. A. Goddard III, "A New Interpretation of the Physical Nature of the Chemical Bond" (to be published)
20. O. J. Sovers, M. Karplus, J. C. P., 44, 3033 (1966)
21. U. Kaldor, J. C. P., 46, 1981 (1967)
22. Experiment only determines the absolute value of the hyperfine splitting constant